

CKM determination from W decays with jet flavor tagging at CEPC

Zhao-Ling Zhang¹ Li-Bo Liao² Jia-Rong Li³ Jia-Bao Gong^{4,5} Wei-Min Song¹
Gang Li^{4,5}

¹College of Physics, Jilin University, Changchun, China

²Sun Yat-sen University, Guangzhou, China

³Tsinghua University, Beijing, China

⁴Institute of High Energy Physics, CAS, Beijing, China

⁵University of Chinese Academy of Sciences, Beijing, China

CEPC Physics Performance Group Meeting
June 1, 2026

Outline

- 1 Motivation
- 2 Analysis setup
- 3 Jet flavor tagging
- 4 Results

Why measure CKM elements with W decays?

- The CKM matrix is the flavor-mixing matrix of the Standard Model.
- Precise measurements test CKM unitarity and probe new physics.
- Hadronic W decays provide a clean electroweak alternative to meson decays.
- The branching fraction is directly related to $|V_{ij}|^2$ with very small hadronic uncertainty.

Key relation

$$\text{BR}(W^- \rightarrow \bar{q}_i q_j) \propto |V_{ij}|^2$$

Why CEPC?

- large $W^+ W^-$ sample at $\sqrt{s} = 240$ GeV
- clean $e^+ e^-$ environment
- strong heavy- and light-flavor tagging capability

Target elements in this study

$|V_{ud}|$, $|V_{us}|$, $|V_{cd}|$, $|V_{cs}|$, and $|V_{cb}|$

Dataset and signal topology

- Signal channel: $e^+e^- \rightarrow W^+W^- \rightarrow \mu\nu\bar{q}q$.
- Simulation at $\sqrt{s} = 240$ GeV with 21.6 ab^{-1} .
- Signal channels considered: ud , us , ub , cd , cs , and cb .
- The ub mode is negligible and is fixed in the fit.
- Dominant backgrounds come from $2f$, ZZ , semileptonic WW , single- W/Z , and ZH processes.

Simulation chain

WHIZARD \rightarrow PYTHIA \rightarrow DELPHES

Main analysis handle

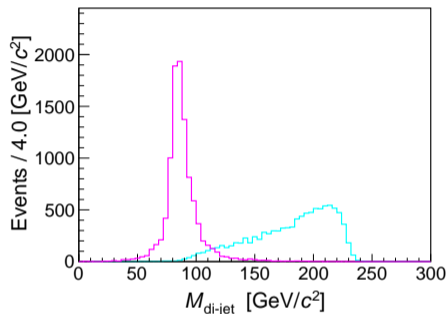
separate the hadronic W decay flavor with jet tagging and binned simultaneous fits

Event picture

one isolated muon + missing momentum + two reconstructed jets

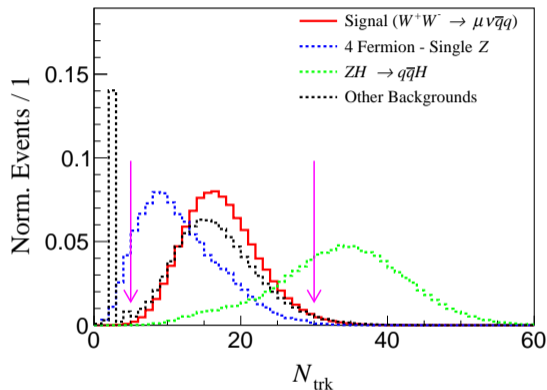
Event selection overview

- Preselection: $5 \leq N_{\text{trk}} \leq 30$,
 $50 \leq \sum E_{\text{trk}} \leq 200 \text{ GeV}$, $P(\gamma_{\text{lead}}) < 60 \text{ GeV}$,
and at least one lepton.
- Muon requirements: $N_{\mu} \geq 1$, $P(\mu_{\text{lead}}) \geq 20 \text{ GeV}$,
 $\sum P(\mu) \leq 100 \text{ GeV}$.
- Kinematics: $80^{\circ} \leq \theta(\mu_{\text{lead}}, \text{di-jet}) \leq 170^{\circ}$
and $E_{\text{ratio}}(\mu_{\text{lead}}) \geq 0.9$.
- Hadronic system: $50 \leq M_{\text{di-jet}} \leq 120 \text{ GeV}$,
 $Y_{23} \leq 0.1$, $Y_{34} \leq 0.008$.
- Global cleanup: $|\cos \theta_{\text{miss}}| < 0.9$, $U_{\text{miss}} \leq 15 \text{ GeV}$,
and $\chi_{\text{IP}}^2 < 10$.

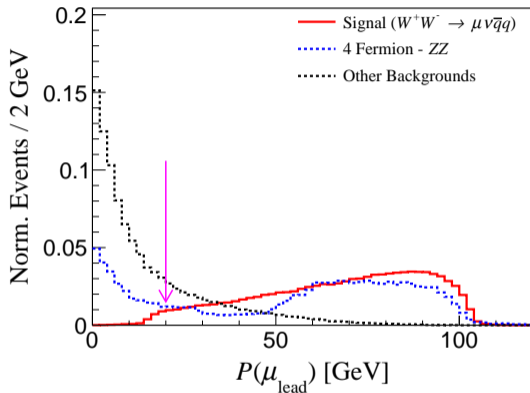


Removing the leading muon before clustering restores the hadronic W mass peak.

Selection variables I

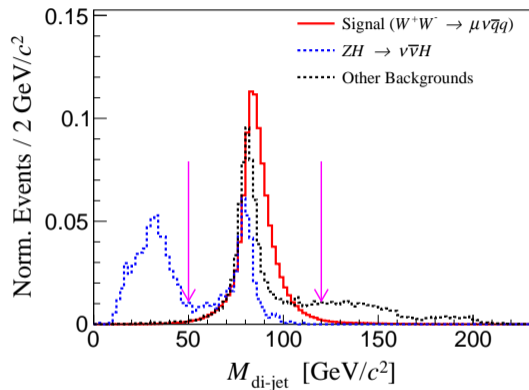


Charged-track multiplicity cleanly rejects low-multiplicity leptonic events.

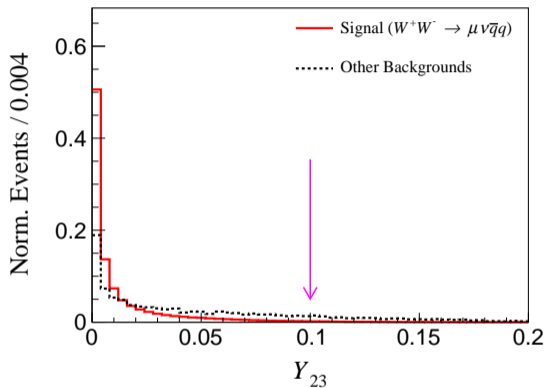


The leading-muon momentum suppresses soft and non-prompt muons.

Selection variables II



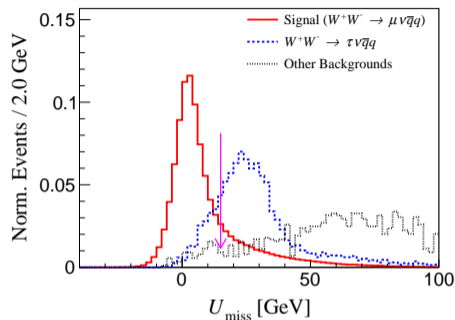
The di-jet mass selects the hadronic W resonance.



The jet-resolution variable rejects residual multi-jet topologies.

Selection variable III

- The missing-momentum direction suppresses ISR-dominated and forward-peaked events.
- The missing-mass proxy $U_{\text{miss}} = E_{\text{miss}} - P_{\text{miss}}$ rejects multi-neutrino backgrounds.
- The final impact-parameter requirement removes cosmic-ray and decay-in-flight contamination.
- After the full selection, the background contamination is reduced to a very small level.



Residual background

Dominated by $W^+W^- \rightarrow \tau\nu\bar{q}q$ with small ZZ and ZH contributions.

Selection cutflow

Selection criterion	$\mu\nu\bar{c}s$	$q\bar{q}$	ZZ	$\tau\nu\bar{q}q$	ZH
Total events	25,257,744	1,168,708,160	9,668,592	57,499,848	4,399,256
$N_{\text{jet}} = 2$	100.0%	99.9%	100.0%	100.0%	93.1%
$5 \leq N_{\text{trk}} \leq 30$	99.0%	94.9%	97.6%	99.6%	47.8%
$N_{\ell} \geq 1$	98.9%	24.3%	54.5%	45.2%	32.3%
$50 \leq \sum E_{\text{trk}} \leq 200$ GeV	97.8%	19.2%	44.7%	42.0%	31.0%
$P(\gamma_{\text{lead}}) \leq 60$ GeV	97.4%	15.5%	43.2%	41.8%	30.9%
$N_{\mu} \geq 1$	97.4%	6.6%	36.7%	19.4%	16.8%
$P(\mu_{\text{lead}}) \geq 20$ GeV	95.1%	1.2%	27.7%	9.8%	5.0%
$\sum P(\mu) \leq 100$ GeV	90.5%	1.2%	10.0%	9.8%	5.0%
$80^{\circ} \leq \theta(\mu_{\text{lead}}, \text{di-jet}) \leq 170^{\circ}$	82.9%	0.2%	3.1%	8.5%	3.3%
$E_{\text{ratio}}(\mu_{\text{lead}}) \geq 0.9$	79.7%	< 0.1%	1.8%	8.2%	2.3%
$50 \leq M_{\text{di-jet}} \leq 120$ GeV	77.8%	< 0.1%	1.0%	7.9%	0.8%
$Y_{23} \leq 0.1$	76.6%	< 0.1%	0.9%	6.5%	0.6%
$Y_{34} \leq 0.008$	73.8%	< 0.1%	0.8%	5.8%	0.4%
$ \cos \theta_{\text{miss}} \leq 0.9$	68.4%	0.0%	0.1%	4.4%	0.4%
$U_{\text{miss}} \leq 15$ GeV	54.1%	0.0%	< 0.1%	0.8%	< 0.1%
$\chi_{\text{IP}}^2 \leq 10$	53.8%	0.0%	< 0.1%	0.2%	< 0.1%
Final expected yields	13,588,666	0	3,846	115,000	1,225

Background categories before and after selection

Before selection	
Category	Events
Signal ($\mu\nu\bar{q}q$)	53,351,568
Two-fermion ($q\bar{q}, \ell\ell, \nu\nu$)	3,090,157,920
ZZ	12,020,184
W^+W^- ($\tau\nu\bar{q}q, e\nu\bar{q}q$)	111,614,328
single- Z	9,971,856
single- W	75,281,400
ZH	4,399,256
Total background	3,303,444,944

After full selection	
Category	Events
Signal ($\mu\nu\bar{q}q$)	29,867,852
Two-fermion ($q\bar{q}, \ell\ell, \nu\nu$)	0
ZZ	3,846
W^+W^- ($\tau\nu\bar{q}q, e\nu\bar{q}q$)	115,000
single- Z	negligible
single- W	negligible
ZH	1,225
Total background	120,071

The surviving background is dominated by $W^+W^- \rightarrow \tau\nu\bar{q}q$, with smaller ZZ and ZH contributions.

Final signal yields after the full selection

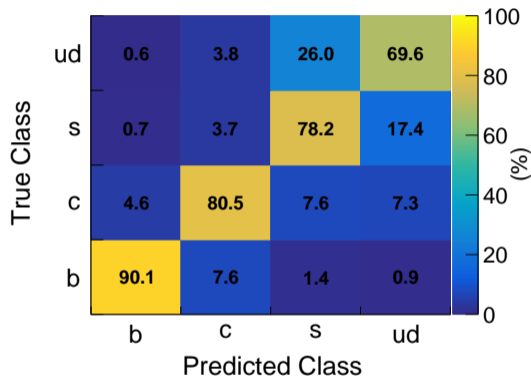
Signal channel	Efficiency (%)	Expected yield
$W^+ W^- \rightarrow \mu\nu\bar{u}d$	58.2	14,746,269
$W^+ W^- \rightarrow \mu\nu\bar{u}s$	56.4	763,958
$W^+ W^- \rightarrow \mu\nu\bar{c}d$	55.2	747,704
$W^+ W^- \rightarrow \mu\nu\bar{c}s$	53.8	13,588,666
$W^+ W^- \rightarrow \mu\nu\bar{c}b$	44.7	21,048
$W^+ W^- \rightarrow \mu\nu\bar{u}b$	48.0	207

Takeaway

The selection keeps more than 50% efficiency for the light and charm channels while strongly suppressing the background.

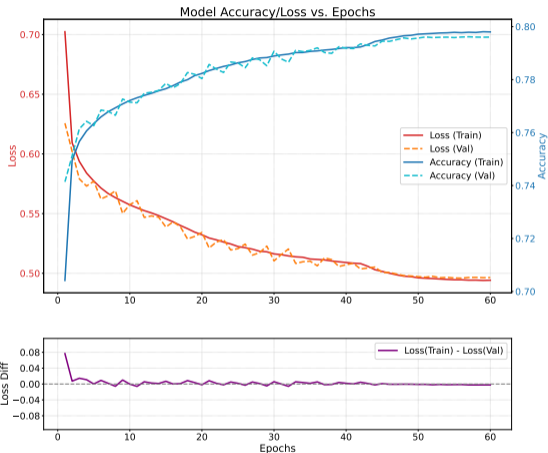
ParticleNet flavor tagger

- Four output classes: b , c , s , and ud .
- The u and d jets are merged because they are experimentally difficult to separate.
- Lightweight architecture: three EdgeConv blocks, 8 nearest neighbors, and a final dense layer.
- Trained with 1M events per class for 60 epochs using Adam.
- Validation accuracy reaches 79.6%.
- The largest residual confusion is between s and ud jets.



Training stability

- Training and validation curves converge smoothly.
- No visible sign of overfitting.
- Best performance is reached after about 50 epochs.



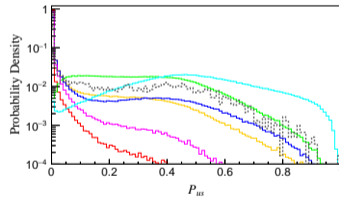
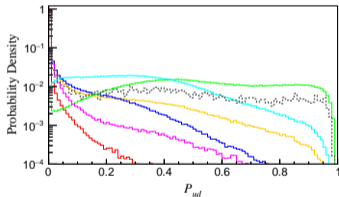
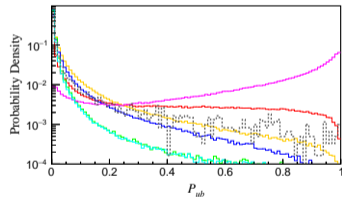
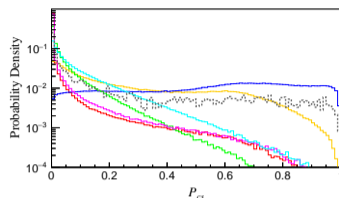
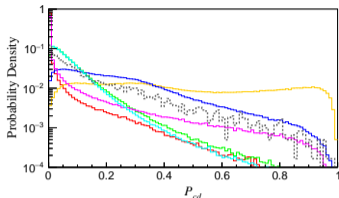
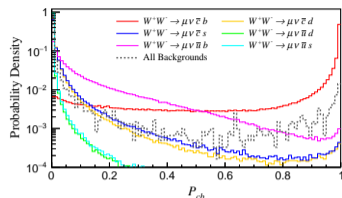
Event-level flavor discriminants

- For each jet pair, the two ParticleNet outputs are combined into an event-level discriminant.
- The six discriminants correspond to the signal hypotheses P_{cb} , P_{cd} , P_{cs} , P_{ub} , P_{ud} , and P_{us} .
- Values near unity indicate a good match to the target flavor assignment.
- Background and mismatched flavor combinations populate smaller values.

$$P_{ij} = \frac{P_1(i)P_2(j)+P_2(i)P_1(j)}{\sum_{h_1, h_2 \in \{b, c, s, ud\}} [P_1(h_1)P_2(h_2)+P_2(h_1)P_1(h_2)]}$$

The symmetrized numerator removes the jet-order ambiguity.

Event-level discriminant shapes



The signal hypothesis is concentrated at large discriminant values, while backgrounds populate the low-discriminant region.

From fitted yields to branching fractions

- The fitted signal yields are converted into branching fractions using the channel efficiency.
- The ub contribution is fixed because its expected yield is negligible.
- The extracted branching fractions provide the direct input for the CKM determination.

Physics point

The conversion is clean because the flavor-independent QCD and electroweak corrections largely cancel in the ratio.

Branching fraction

$$\text{BR}(W^- \rightarrow \bar{q}_i q_j) = \frac{N_{ij}}{\varepsilon_{ij} \cdot N_{W^+ W^- \rightarrow \mu\nu \bar{q}q}}$$

From branching fractions to CKM elements

- Under CKM unitarity, the hadronic W branching fraction gives a direct handle on $|V_{ij}|$.
- The simultaneous fit result is translated channel by channel into the CKM elements.

CKM relation

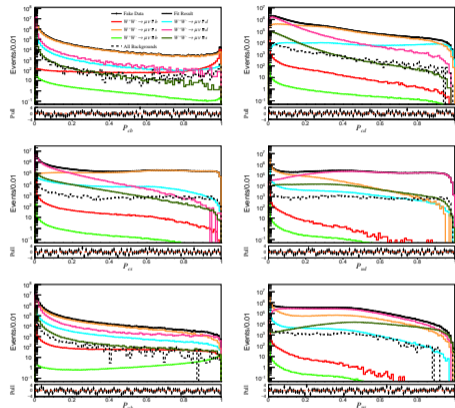
$$|V_{ij}| \approx \sqrt{\frac{2N_{ij}}{\epsilon_{ij} \cdot N_{W^+W^- \rightarrow \mu\nu\bar{q}q}}}$$

Interpretation

This gives an electroweak determination of CKM elements without hadronic form-factor uncertainties.

Binned simultaneous fit and CKM extraction

- Event-level flavor discriminants are built from the two jet-tag outputs.
- A binned simultaneous fit is performed for the six hypotheses P_{cb} , P_{cd} , P_{cs} , P_{ub} , P_{ud} , and P_{us} .
- The selected sample is large, so a binned extended maximum-likelihood fit is used.
- The ub contribution and the residual background are fixed.
- Fitted yields agree well with the input expectations.



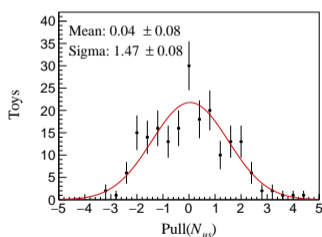
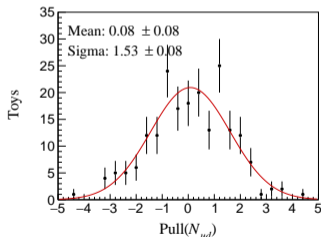
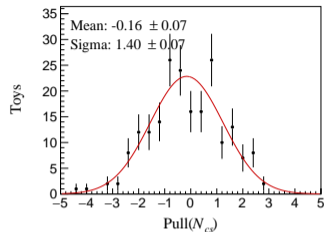
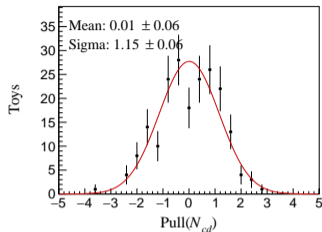
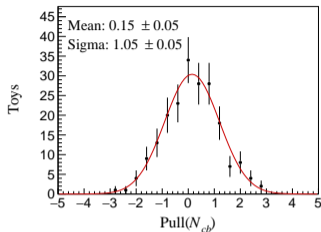
Fitted yields

Yield	Initial	Fitted	Uncertainty	Rel. unc.
N_{cb}	2.10×10^4	2.12×10^4	2.50×10^2	1.18%
N_{cd}	7.48×10^5	7.45×10^5	2.66×10^3	0.36%
N_{cs}	1.36×10^7	1.36×10^7	3.22×10^3	0.02%
N_{ud}	1.47×10^7	1.48×10^7	3.40×10^3	0.02%
N_{us}	7.64×10^5	7.61×10^5	3.09×10^3	0.41%

The fitted yields are consistent with the input expectations.

- The pull study is shown on the next slide.
- High-yield channels dominate the statistical precision.

Pull validation



Pull means are compatible with zero and the widths are close to unity.

Statistical uncertainty

- Statistical uncertainties come directly from the binned simultaneous fit.
- For each channel, the relative statistical uncertainty on $|V_{ij}|$ follows

$$\frac{\delta|V_{ij}|}{|V_{ij}|} = \frac{1}{2} \frac{\delta N_{ij}}{N_{ij}}.$$

- The relative yield uncertainties range from 0.02% to 1.18% for the fitted channels.
- The smallest statistical errors come from the high-yield *ud* and *cs* modes.

Systematic uncertainty

- Detector resolution effects are evaluated by varying the track, vertex, and calorimeter resolutions by $\pm 10\%$.
- The common detector-related uncertainty is 0.82% and dominates the quoted total precision.
- Parton-shower and hadronization modeling are important for a full analysis, but are not included in the quoted total here.
- Flavor-tag calibration and external unitarity input are also treated as future or interpretation-level uncertainties.

Quoted total uncertainty

$$\sigma_{\text{tot}} = \sqrt{\sigma_{\text{stat}}^2 + \sigma_{\text{syst}}^2}$$

Main message

The quoted total uncertainty is dominated by detector-driven systematics rather than by statistics.

Projected precision on CKM elements

CKM element	CEPC total	PDG avg.	Benchmark
$ V_{ud} $	0.83%	0.03%	PIBETA: 0.28%
$ V_{us} $	0.84%	0.38%	KLOE: 0.18%
$ V_{cd} $	0.84%	1.81%	BESIII: 3.4%
$ V_{cs} $	0.83%	0.62%	BESIII: 1.7%
$ V_{cb} $	1.02%	2.92%	Belle-based: 1.5%

- The CEPC is competitive for $|V_{cd}|$, $|V_{cs}|$, and $|V_{cb}|$.
- It provides an independent electroweak determination for all five CKM elements.

Summary

- We studied direct CKM measurements from semileptonic W decays at the CEPC.
- A clean event selection and ParticleNet-based jet flavor tagging provide strong flavor separation.
- A binned simultaneous fit yields projected precisions of 0.83–1.02% for the five CKM elements studied.
- The CEPC can provide competitive and complementary CKM measurements in a clean electroweak environment.
- **Current Status:** The manuscript draft has been prepared.
- **Next Steps:** Investigate the pull width issue and check the Toy MC generation.

Thank you!